Hesperidin inhibits tobacco smoke-induced pulmonary cell proliferation and EMT in mouse lung tissues via the p38 signaling pathway

ZHAOFENG LIANG[1*], YUE ZHANG[1*], YUMENG XU[1], XINYI ZHANG[1] and YANAN WANG[2]

[1]Jiangsu Key Laboratory of Medical Science and Laboratory Medicine, School of Medicine, Jiangsu University, Zhenjiang, Jiangsu 212013; [2]Department of Clinical Laboratory, The Affiliated Suzhou Hospital of Nanjing Medical University, Suzhou Municipal Hospital, Gusu School, Suzhou, Jiangsu 215002, P.R. China

Received August 12, 2022; Accepted November 11, 2022

DOI: 10.3892/ol.2022.13616

Abstract. Tobacco smoke (TS) is the major cause of lung cancer. The abnormal proliferation and epithelial-mesenchymal transition (EMT) of lung cells promote occurrence and development of lung cancer. The p38 pathway intervenes in this cancer development. Hesperidin also serves a role in human health and disease prevention. The roles of p38 in TS-mediated abnormal cell proliferation and EMT, and the hesperidin intervention thereof are not yet understood. In the present study, it was demonstrated that TS upregulated proliferating cell nuclear antigen, vimentin and N-cadherin expression, whereas it downregulated E-cadherin expression, as assessed using western blotting and reverse transcription-quantitative PCR. Furthermore, it was observed that inhibition of the p38 pathway inhibit TS-induced proliferation and EMT. Hesperidin treatment prevented the TS-induced activation of the p38 pathway, EMT and cell proliferation in mouse lungs. The findings of the present study may provide insights into the pathogenesis of TS-related lung cancer.

Correspondence to: Professor Zhaofeng Liang, Jiangsu Key Laboratory of Medical Science and Laboratory Medicine, School of Medicine, Jiangsu University, 301 Xuefu Road, Zhenjiang, Jiangsu 212013, P.R. China
E-mail: liangzhaofeng@ujs.edu.cn

Dr Yanan Wang, Department of Clinical Laboratory, The Affiliated Suzhou Hospital of Nanjing Medical University, Suzhou Municipal Hospital, Gusu School, 16 Baita West Road, Suzhou, Jiangsu 215002, P.R. China
E-mail: wangyn1980@163.com

*Contributed equally

Key words: lung cancer, hesperidin, tobacco smoke, intervention, p38

Introduction

Lung cancer is one of the most common causes of cancer-related deaths in men and women worldwide (1,2). Tobacco smoke (TS) is associated with multiple types of cancer, but especially lung cancer (3,4). Epidemiological studies have revealed a link between TS and lung cancer initiation and development (5-7). TS accounts for 80% of female and 90% of male lung cancer cases (8,9). Lung cancer contributes to >3,000 deaths per day and is the leading cause of cancer-related deaths in men and women (2). However, the molecular pathogenesis of TS-induced lung cancer still remains largely unknown.

Lung cancer is a multicentric and multistep phenomenon, which sequentially accumulates molecular and genetic abnormalities (9). Abnormal cell proliferation and epithelial-mesenchymal transition (EMT) help in developing lung cancer and can be activated by carcinogens (10-12). It has been demonstrated that exposure of cells or mice to TS accelerates the EMT process, which is characterized by changes in the expression of EMT markers, including decreased E-cadherin, and increased vimentin and N-cadherin (13-15). In addition, TS-induced EMT initiates early-stage carcinogenesis (16-18). Cancer is a group of diseases characterized by abnormal cell proliferation, and abnormal cell proliferation is a key step that may promote the occurrence and development of cancer (19-22). Studies have suggested that exposure to TS induces abnormal cell proliferation accompanied by changes in the expression of PCNA or Ki-67 (23-25). To the best of our knowledge, the molecular mechanism of TS-induced abnormal pulmonary cell proliferation and EMT is unclear. However, further investigations may provide strategies for early treatment and intervention in lung cancer.

MAPKs control cellular processes, such as proliferation, apoptosis, angiogenesis, cell motility and differentiation (26,27). Therefore, MAPKs can contribute to tumorigenesis (28-30). p38 is a member of the MAPK family, participating in the occurrence and development of TS-induced lung cancer by regulating the EMT process (30-36). However, the functional mechanism of p38 in lung tissues is not clear.

Dietary phytochemicals are potentially anticancerous and flavonoids have been reported to inhibit cancer progression (37). Hesperidin is a citrus flavone, which is the abundant polyphenol in citrus fruits and is commonly used in Traditional Chinese Medicine (37,38). Hesperidin exerts a range of biological and pharmacological activities, including antioxidant, anti-inflammatory and anticancer effects, with minimal or no side effects (39-41). Hesperidin is anticancerous for tumors, such as breast, gastric and lung tumors. The anticancer activity of hesperidin has been well studied (37,39,42,43). However, limited work has been conducted on its potential to treat TS-induced abnormal cell proliferation and EMT in lung tissues.

The present study examined the regulation of the p38 pathway in TS-induced abnormal lung cell proliferation and EMT. The preventive effects of hesperidin were determined by examining the lung tissues of treated mice. The findings may provide a novel avenue for determining the pathogenesis and early interventions of TS-induced lung tumorigenesis.

Table I. Primer sequences.

Gene name	Primer sequence (5'-3')
E-cadherin	Forward: CAGGTCTCCTCATGGCTTTGC
	Reverse: CTTCCGAAAAGAAGGCTGTCC
PCNA	Forward: CAAGAAGGTGTTGGAGGCA
	Reverse: TCGCAGCGGTAGGTGTC
Vimentin	Forward: CCTTGACATTGAGATTGCCA
	Reverse: GTATCAACCAGAGGGAGTGA
N-cadherin	Forward: TCAGGCGTCTGTAGAGGCTT
	Reverse: ATGCACATCCTTCGATAAGACTG
GAPDH	Forward: AGGTCGGTGTGAACGGATTTG
	Reverse: TGTAGACCATGTAGTTGAGGTCA

PCNA, proliferating cell nuclear antigen.

Materials and methods

Chemicals and reagents. Phosphorylated p38 (catalogue number, 4511T; 1:500), phosphorylated c-Fos (catalogue number, 5348T; 1:1,000), p38 (catalogue number, 8690T; 1:1,000), c-Fos (catalogue number, 2250T; 1:1,000), E-cadherin (catalogue number, 3195T; 1:1,000) and N-cadherin (catalogue number, 13116T; 1:1,000) antibodies were purchased from Cell Signaling Technology, Inc. Vimentin (catalogue number, MB65651; 1:1,000), proliferating cell nuclear antigen (PCNA) (catalogue number, MB0156; 1:500) and GAPDH (catalogue number, BS65483M; 1:2,000) antibodies were purchased from Bioworld Technology, Inc. Horseradish peroxidase-conjugated secondary antibodies were purchased from Invitrogen; Thermo Fisher Scientific, Inc. (catalogue numbers, 31430 and 31460; 1:2,000). Primers for Vimentin, E-cadherin, N-cadherin, PCNA and GAPDH (Table I) were synthesized by Invitrogen; Thermo Fisher Scientific, Inc. SB203580 was purchased from MilliporeSigma. The sources of other materials are indicated throughout the text.

Mice and exposure to TS. Male 8-week-old BALB/c mice weighing 18-22 g (n=60) were purchased from the Animal Research Center of Jiangsu University (Zhenjiang, China). Mice were acclimated for 1 week prior to TS exposure. The mice were housed in polypropylene cages at 22±0.5˚C and 40-60% humidity with 12 h light/dark cycles at the Animal Care Facility of Jiangsu University (Zhenjiang, China). Water and a normal diet were provided *ad libitum*. All of the mouse experiments were approved by the Animal Care and Use Committee of Jiangsu University and efforts were made to minimize suffering and distress. Mice in the TS group (n=18) were exposed in the smoking apparatus (Beijing Huironghe Technology Co., Ltd.) for 6 h daily for 12 weeks. The filtered air (FA) control group (n=18) mice were exposed to filtered air in the smoking apparatus. After TS exposure, mice in each group were provided with water and a normal diet. Filter-less 3R4F Kentucky reference cigarettes (containing 9.4 mg tar and 0.76 mg nicotine per cigarette) were used as the TS source. In the TS + DMSO group (n=12), mice were injected with sterile DMSO (catalogue number, D2650; MilliporeSigma) and exposed to TS, while in the TS + SB203580 group (n=6), mice were injected with SB203580 (1 mg/kg body weight) and exposed to TS. SB203580 was dissolved in sterile DMSO and administered intraperitoneally every other day. In the TS + hesperidin group (n=6), mice were exposed to TS and received 30 mg/kg hesperidin (catalogue number, HY-15337; MedChemExpress) every other day by gavage, and a normal diet. SB203580 and hesperidin were dissolved in DMSO, and further diluted in 0.9% saline to the final concentration. TS was generated by a smoke machine, which pumped the smoke from the burning cigarette at a constant rate (5 min/cigarette). Smoke was delivered to the whole-body exposure chambers with total particulate matter (TPM) of 85 mg/m^3. The exposures were monitored and characterized as: Carbon monoxide (16.75±2.47 ppm) and TPM (0 mg/m^3) for the control group; and carbon monoxide (181.05±14.79 ppm) and TPM (84.83±5.19 mg/m^3) for the TS exposure group. Animal health and behavior were monitored twice a week and the experiment lasted for 12 weeks. There was no accidental death of mice during the experiment, and all mice were euthanized at the end of the experiment. Mice were sacrificed by cervical dislocation and death was confirmed by the sound of cervical spine fracture and the absence of breathing (44).

Western blot analysis. Lung tissues were homogenized using a full automatic sample rapid grinding instrument (Shanghai Jingxin Industrial Development, Co., Ltd.) in lysis buffer containing 1X protease inhibitor cocktail (Pierce; Thermo Fisher Scientific, Inc.) and centrifuged at 12,000 x g at 4˚C for 15 min. Protein concentration was determined by bicinchoninic acid assay. Equal amounts of proteins (60 μg) were fractionated by electrophoresis via 7.5-10% SDS-PAGE and transferred to a PVDF membrane (MilliporeSigma). The membrane was blocked using 5% non-fat milk at 25˚C for 1 h and incubated overnight with monoclonal antibody at 4˚C. The membranes were washed with tris-buffered saline with 0.1% Tween-20 and probed with horseradish peroxidase-conjugated secondary antibody diluted in 5% skimmed milk. GAPDH

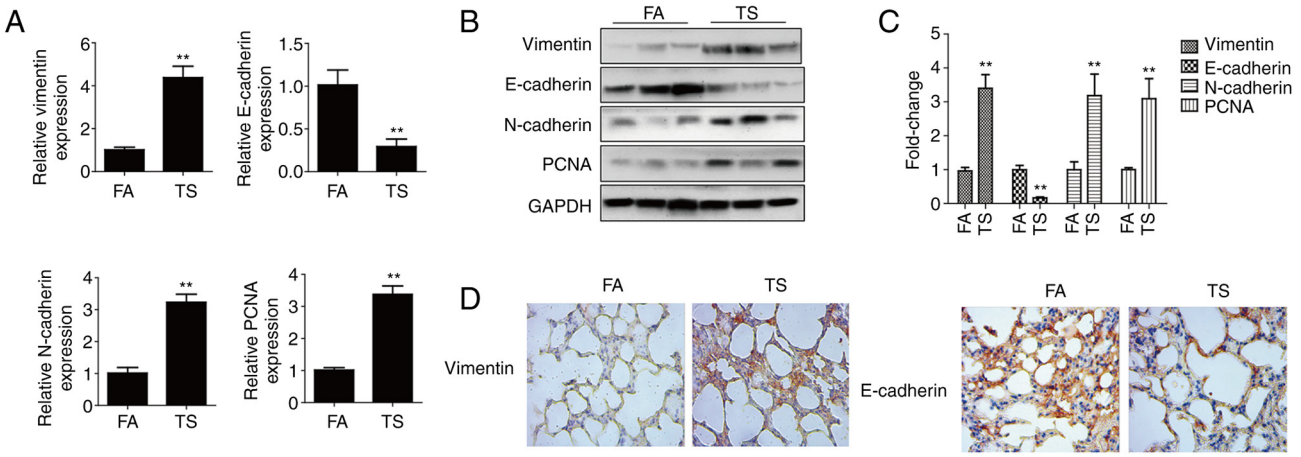

Figure 1. TS-induced abnormal EMT and cell proliferation processes in mouse lung tissues. Mice were exposed to TS or FA daily for 6 h for a total of 12 weeks. (A) TS reduced mRNA levels of the epithelial marker (E-cadherin) and increased mesenchymal and proliferation marker levels. (B) TS induced alterations in the protein expression levels of EMT and proliferation markers. (C) Densitometric analyses of western blotting for E-cadherin, vimentin, N-cadherin and PCNA. (D) Immunohistochemistry revealed decreased E-cadherin expression and increased vimentin expression after exposure to TS (magnification, x40). **P<0.01 compared with FA. The error bars shown in the graphs indicate the standard deviation. EMT, epithelial-mesenchymal transition; FA, filtered air; PCNA, proliferating cell nuclear antigen; TS, tobacco smoke.

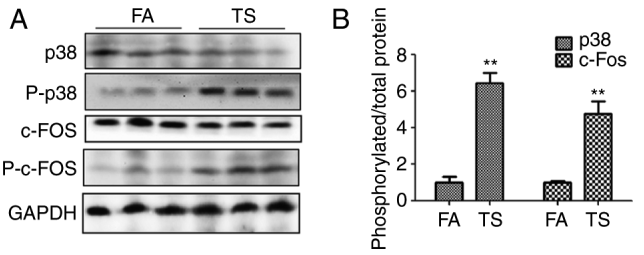

Figure 2. TS increases p38 pathway activation in mouse lung tissues. Mice were exposed to TS or FA for 6 h daily for a total of 12 weeks. (A) Western blotting was used to detect the effect of 12 weeks of TS exposure on the expression of p38, c-Fos, p-p38 and p-c-Fos. (B) Evaluation of the phosphorylated protein/total protein ratio by density analysis of western blotting. **P<0.01 compared with FA. The error bars shown in the graphs indicate the standard deviation. FA, filtered air; p-, phosphorylated; TS, tobacco smoke.

served as the loading control. The membranes were developed with ECL kit (catalogue number, E412-02; Vazyme Biotech Co., Ltd.). For densitometric analyses, protein bands on the blots were measured with ImageJ 1.8.0.345 (National Institutes of Health).

Reverse transcription-quantitative PCR (RT-qPCR). Total RNA from the lung tissues of the mice was isolated using TRIzol™ (Gibco; Thermo Fisher Scientific, Inc.). A total of 2 μg RNA was reverse transcribed into cDNA using AMV Reverse Transcriptase (Promega Corporation) and the HiScript® III 1st Strand cDNA Synthesis Kit (catalogue number, R312-01; Vazyme Biotech Co., Ltd.) was used according to the manufacturer's protocol. qPCR was performed using AceQ® qPCR SYBR Green Master Mix (Vazyme Biotech Co., Ltd.) and a StepOnePlus™ Real-Time PCR System (Applied Biosystems; Thermo Fisher Scientific, Inc.). The thermocycling conditions were as follows: 95˚C for 5 min, followed by 40 cycles at 95˚C for 15 sec, 60˚C for 15 sec, 72˚C for 20 sec and a 65-95˚C drawing dissociation curve (45). GAPDH expression was used as the normalization control. Fold-changes in the expression of each gene were calculated using the $2^{-\Delta\Delta Cq}$ (46). The primers used are shown in Table I.

Immunohistochemistry. Immunohistochemistry was performed according a previously reported method (47). Briefly, tissues were fixed in 4% buffered formalin at room temperature for 24 h. 5-μm paraffin-embedded continuous sections were de-waxed in xylene and rehydrated in graded alcohol. Next, the endogenous peroxidase activity was quenched by incubating the slices in 3% (v/v) H_2O_2 in methanol. Antigen-retrieval was performed by incubating the sections in citrate buffer (pH 6.0) and the non-specific binding was blocked using 5% bovine serum albumin at 37˚C for 30 min. After incubation overnight with E-cadherin (catalogue number, 3195T; 1:200; Cell Signaling Technology, Inc.) and Vimentin (catalogue number, MB9006; 1:100; Bioworld Technology, Inc.) at 4˚C, the sections were subsequently washed with phosphate-buffered solution, and then incubated with biotinylated immunoglobulin G and SABC (catalogue number, SA1020; Wuhan Boster Biological Technology, Ltd.) for 1 h. Image acquisition was performed with a light microscope (Nikon Solar Eclipse Ti-S; Nikon Corporation).

Statistical analysis. Statistical analysis was performed using SPSS 16.0 (SPSS, Inc.). The data of three repeated experiments are presented as the mean ± standard deviation. One-way ANOVA, followed by Tukey's post hoc test, was used to analyze the statistical differences among multiple groups. The differences between two groups were analyzed using an unpaired t-test. P<0.05 was considered to indicate a statistically significant difference.

Results

TS-induced abnormal EMT and cell proliferation in mouse lung tissues. TS is the dominant risk factor for lung

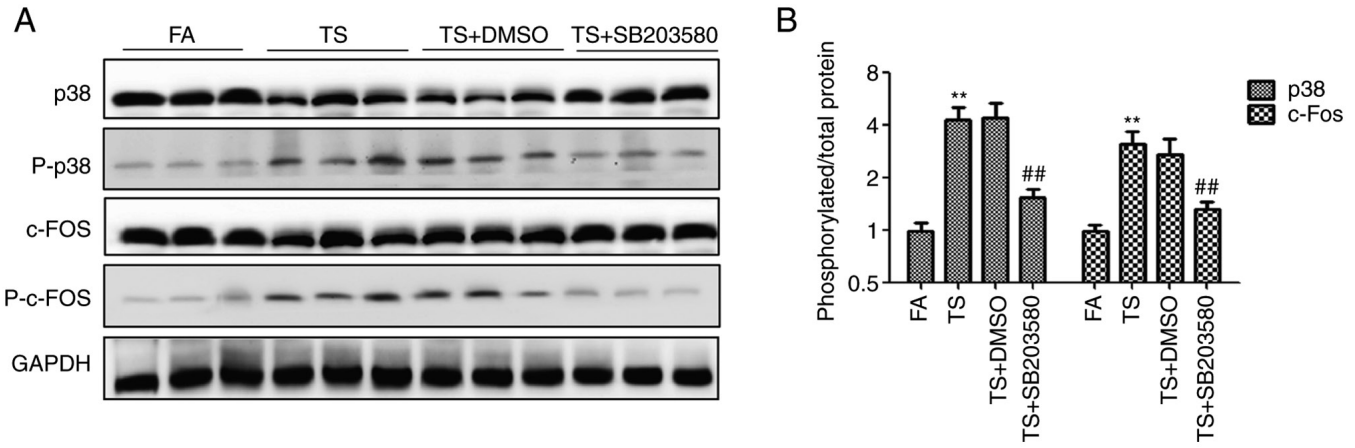

Figure 3. SB203580 inhibits TS-induced p38 pathway activation. Mice were treated with FA, TS, TS + DMSO or TS + SB203580 for 12 weeks. (A) Western blot analysis revealed that SB203580 inhibited the TS-induced changes of p-p38 and p-c-Fos. (B) Evaluation of the phosphorylated protein/total protein ratio by density analysis of western blotting. **P<0.01, compared with the FA control; $^{\#\#}$P<0.01, compared with TS alone. The error bars shown in the graphs indicate the standard deviation. FA, filtered air; p-, phosphorylated; TS, tobacco smoke.

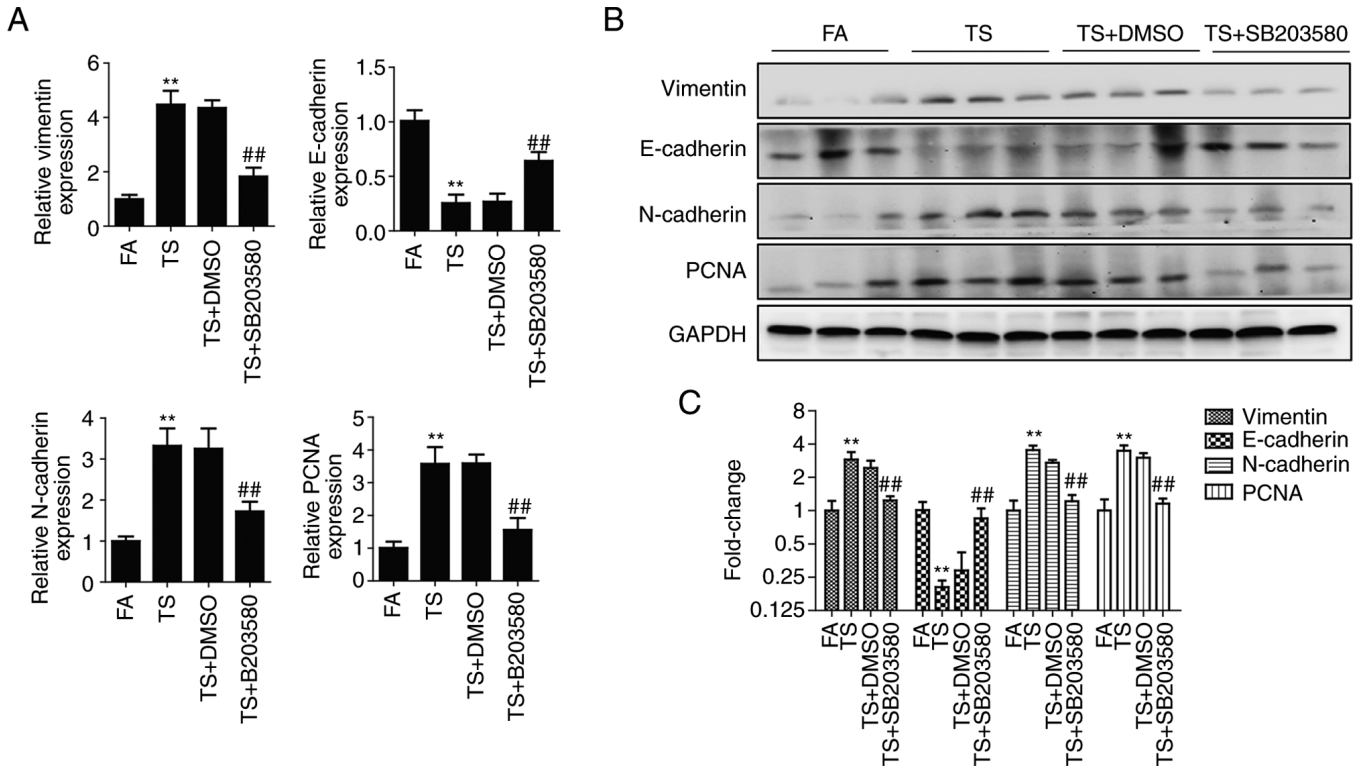

Figure 4. TS-mediated abnormal EMT and cell proliferation are prevented by inhibition of the p38 pathway. Mice were treated with FA, TS, TS + DMSO or TS + SB203580 for 12 weeks. (A) Reverse transcription-quantitative PCR was used to analyze the expression levels of EMT and cell proliferation markers. (B) Western blotting was used to analyze the levels of EMT and cell proliferation markers, which were (C) semi-quantified. **P<0.01, compared with the FA control; $^{\#\#}$P<0.01, compared with TS only. The error bars shown in the graphs indicate the standard deviation. EMT, epithelial-mesenchymal transition; FA, filtered air; PCNA, proliferating cell nuclear antigen; TS, tobacco smoke.

cancer (3,4). Abnormal EMT and cell proliferation initiate TS-induced lung cancer (16,25). The altered EMT and cell proliferation marker (E-cadherin, vimentin, N-cadherin and PCNA) levels were screened in mouse lung tissues after 12 weeks of TS exposure. The RT-qPCR results showed a reduction in E-cadherin mRNA levels after TS exposure compared with the levels in the FA control group, whereas vimentin, N-cadherin and PCNA levels were elevated (Fig. 1A). The western blotting results revealed that TS reduced E-cadherin protein expression compared with that in the FA group, but increased vimentin, N-cadherin and PCNA expression (Fig. 1B and C). In order to further clarify that smoking can induce EMT in lung tissue of mice, vimentin and E-cadherin were detected by immunohistochemistry. It was demonstrated that TS increased vimentin expression but decreased E-cadherin expression compared

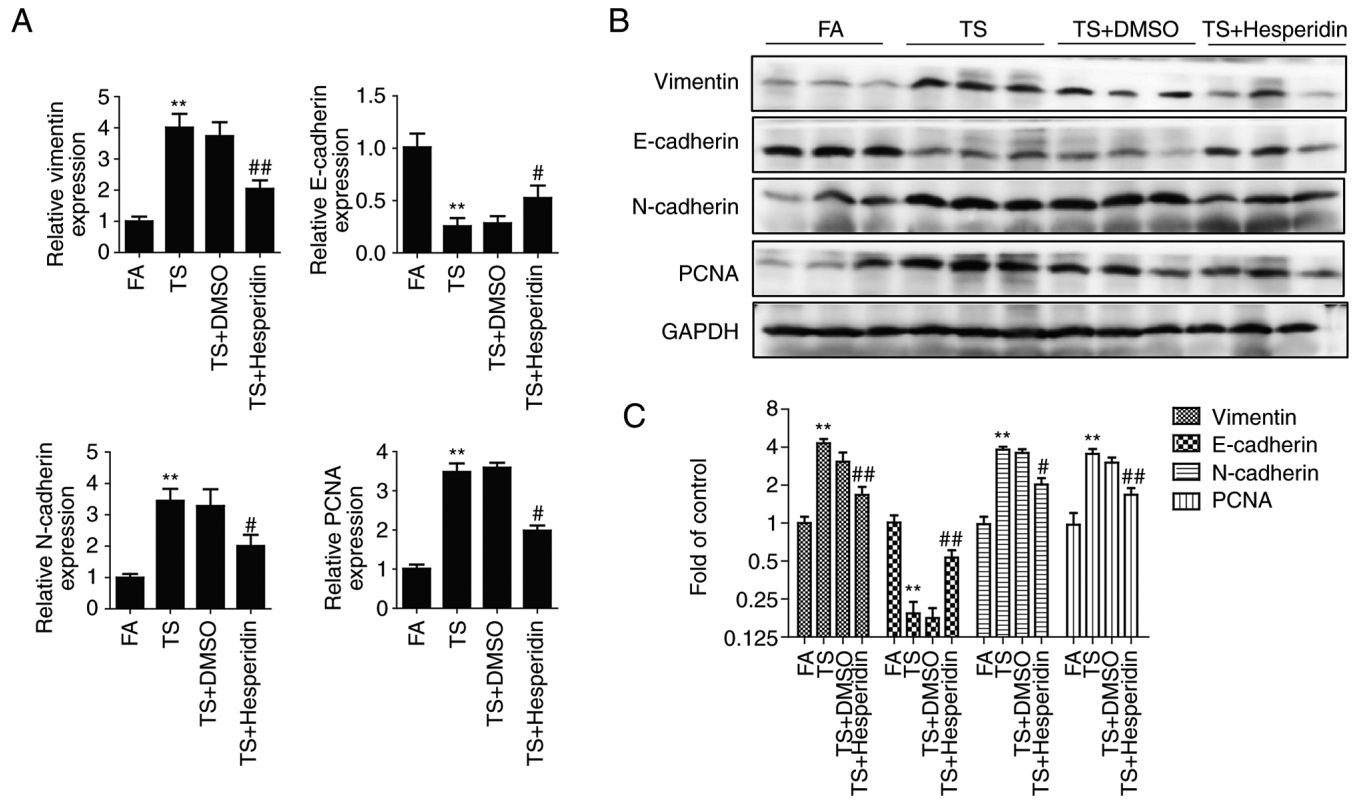

Figure 5. Hesperidin inhibits the abnormal EMT and cell proliferation in lung tissues from mice exposed to TS. Mice were treated with FA, TS, TS + DMSO and TS + hesperidin for 12 weeks. (A) Reverse transcription-quantitative PCR was used to analyze the mRNA levels of EMT and proliferation markers. (B) Protein expression levels of EMT and proliferation markers were analyzed by western blotting and (C) semi-quantified. **P<0.01, compared with FA; $^{\#}$P<0.05, $^{\#\#}$P<0.01, compared with TS only. The error bars shown in the graphs indicate the standard deviation. EMT, epithelial-mesenchymal transition; FA, filtered air; PCNA, proliferating cell nuclear antigen; TS, tobacco smoke.

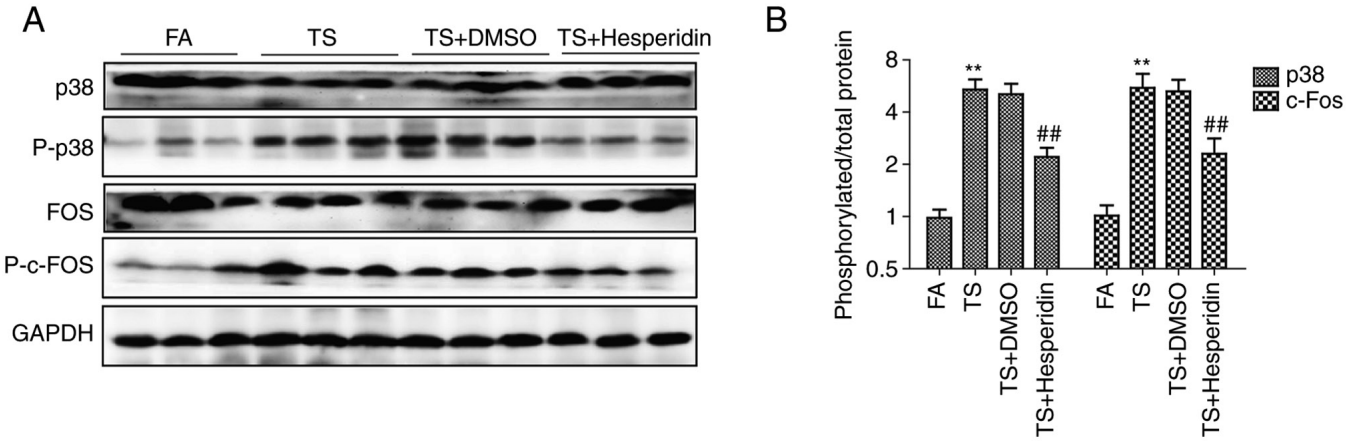

Figure 6. Hesperidin attenuates activation of the p38 pathway by TS. Mice were treated with FA, TS, TS + DMSO and TS + hesperidin for 12 weeks. (A) Western blotting was used to analyze the expression changes of p38, c-Fos, p-p38 and p-c-Fos. (B) Evaluation of the phosphorylated protein/total protein ratio by density analysis of western blotting. **P<0.01, compared with FA; $^{\#\#}$P<0.01, compared with TS only. The error bars shown in the graphs indicate the standard deviation. FA, filtered air; p-, phosphorylated; TS, tobacco smoke.

with that in the FA group (Fig. 1D). Therefore, TS exposure induced abnormal EMT and cell proliferation in mouse lung tissues.

TS-mediated abnormal EMT and cell proliferation are inhibited by p38 pathway inhibition. To determine whether the abnormal lung EMT and proliferation processes triggered by TS are associated with the p38 pathway, the levels of p38, phosphorylated p38 and phosphorylated c-fos in mouse lung tissues were investigated. The western blotting results revealed an increase in phosphorylated p38 and phosphorylated c-Fos levels upon TS exposure compared with that in the FA group (Fig. 2A). In addition, the ratio of phosphorylated protein to total protein was also evaluated, and TS was shown to increase the ratio of phosphorylated p38 and phosphorylated c-Fos compared with the FA group (Fig. 2B).

To further verify the role of p38 pathway, BALB/c mice were treated with SB203580. After 12 weeks of treatment with SB203580, the upregulation of phosphorylated p38 and phosphorylated c-Fos induced by TS was significantly inhibited, as demonstrated by western blotting (Fig. 3A). In addition, the ratio of phosphorylated protein to total protein evaluated by density analysis showed that SB203580 reduced the proportion of the TS-induced increase in phosphorylated p38 and phosphorylated c-Fos (Fig. 3B).

The expression of EMT and proliferation markers was also detected after 12 weeks treatment. These results showed that alterations in the levels of EMT and proliferation markers induced by TS were significantly suppressed by inhibition of the p38 pathway in mouse lung tissues (Fig. 4). Therefore, TS-mediated abnormal EMT and cell proliferation were inhibited by the inhibition of the p38 pathway as shown in the *in vivo* experiments in mice.

Hesperidin inhibits abnormal EMT and cell proliferation in mouse lung tissues elicited by TS. BALB/c mice were administered with hesperidin and exposed to TS for 12 weeks. The downregulation of E-cadherin was reduced, and the upregulation of vimentin, N-cadherin and PCNA was reduced compared with that in the TS group (Fig. 5). The preventive effects of hesperidin on TS-mediated abnormal EMT and cell proliferation in mouse lung tissues were evident.

The effect of hesperidin on TS-induced abnormal pulmonary EMT and cell proliferation through its effects on the p38 pathway was also studied. It was found that hesperidin (30 mg/kg) reversed the increased expression of phosphorylated p38 and phosphorylated c-fos induced by TS (Fig. 6A). In addition, the ratio of phosphorylated protein to total protein evaluated by density analysis showed that hesperidin reduced the phosphorylation level of p38 and c-Fos compared with that in the TS group (Fig. 6B).

Discussion

TS is the leading cause of lung cancer and promotes initiation and progression of pulmonary tumorigenesis (5-7,9,48). The underlying molecular mechanism of TS causing lung cancer remains unclear. The present study focused on TS-induced abnormal EMT and cell proliferation in mouse lungs. The study demonstrated that the p38 pathway regulates TS-associated abnormal pulmonary EMT and cell proliferation. The data presented in the present study indicated that hesperidin suppressed the p38 pathway to prevent TS-induced abnormal pulmonary EMT and cell proliferation. The findings provide insights into the molecular mechanisms of TS-mediated pulmonary tumorigenesis, and provide potential targets for lung cancer intervention.

It is well known that both normal cells and cancer cells can proliferate, but the proliferation of cancer cells is abnormal and uncontrolled (48,49). Antiproliferative activity can inhibit the proliferation of all cells, while antitumor activity only targets cancer cells with abnormal proliferation and has little effect on normal cells. EMT is a common cellular process where cells lose epithelial properties and acquire mesenchymal properties (50,51). Normal cells can acquire EMT properties, which may be an important feature in the carcinogenic process (51). The tumor cell EMT process is a strategy of 'immune escape' and a means to improve invasion and metastasis (52,53). Carcinogens can stimulate abnormal cell proliferation and EMT, leading to lung cancer (10-12). TS-induced abnormal EMT and cell proliferation regulate early events in cancer (54-56). In the present study, the change in the expression levels of EMT and proliferation markers indicated abnormal EMT and cell proliferation in the lungs of mice exposed to TS. This was demonstrated through western blot analysis and RT-qPCR where reduced levels of E-cadherin, and increased levels of vimentin, N-cadherin and PCNA were observed. Immunohistochemical staining also revealed increased vimentin expression and decreased E-cadherin expression.

A number of signaling pathways control abnormal EMT and cell proliferation, including the Wnt/β-catenin, MAPK and NF-κB signaling pathways (57-59). The MAPK pathway regulates physiological processes and pathologies, such as cell proliferation, apoptosis, inflammation, cell motility, differentiation and tumorigenesis (60,61). p38 is an important member of the MAPK family and participates in the development of cancer by regulating EMT and abnormal cell proliferation (30,31,62). The present study demonstrated that TS-mediated abnormal pulmonary EMT and cell proliferation were associated with the upregulation of phosphorylated p38 and phosphorylated c-Fos.

The role of the p38 pathway in abnormal pulmonary EMT and cell proliferation has been previously studied. In these studies, mice were treated with SB203580, which inhibited p38 activation (63,64). In the present study, SB203580 inhibited the upregulation of phosphorylated p38 and phosphorylated c-Fos induced by TS. The suppressed p38 pathway inhibited TS-mediated abnormal pulmonary EMT and cell proliferation, as shown by elevated E-cadherin levels and decreased vimentin, N-cadherin and PCNA levels.

Dietary phytochemicals, such as hesperidin, are considered to contribute to cancer prevention (37,38). The safety of hesperidin and its anticancer activity have been previously demonstrated (41,65,66). The intervention of hesperidin in TS-induced abnormal pulmonary EMT and cell proliferation is through the p38 pathway, where phosphorylated p38 and phosphorylated c-Fos are attenuated by hesperidin.

The results of the present study illustrated that the p38 pathway positively regulated TS-induced abnormal pulmonary EMT and proliferation. The interventive effects of hesperidin were demonstrated, which may aid the understanding of the mechanisms and chemoprevention of TS-induced lung cancer.

Acknowledgements

The authors would like to thank Professor Caiyun Zhong (Nanjing Medical University, Nanjing, China) for providing guidance on mouse model construction and research design.

Funding

The present study was supported by the project of Social Development in Zhenjiang (grant no. SH2021045), the Foundation for Excellent Young Teachers of Jiangsu University (grant no. 5521280013), and Zhenjiang Key Laboratory of

High Technology Research on Exosomes Foundation and Transformation Applications (grant no. SS2018003).

Availability of data and materials

The datasets used and/or analyzed during the current study are available from the corresponding author on reasonable request.

Authors' contributions

ZL, YW and YZ designed the study and wrote, revised the manuscript. YZ and YX performed the experiments. XZ and YX analyzed the data. All authors read and approved the final manuscript. ZL and YW confirm the authenticity of all the raw data.

Ethics approval and consent to participate

Mice were handled as per the guidelines of the Animal Care and Welfare Committee of Jiangsu University (Zhenjiang, China). The study protocol was approved by the Committee on the Ethics of Animal Experiments of Jiangsu University (Zhenjiang, China).

Patient consent for publication

Not applicable.

Competing interests

The authors declare that they have no competing interests.

References

1. Alexander M, Kim SY and Cheng H: Update 2020: Management of non-small cell lung cancer. Lung 198: 897-907, 2020.
2. Sung H, Ferlay J, Siegel RL, Laversanne M, Soerjomataram I, Jemal A and Bray F: Global cancer statistics 2020: GLOBOCAN estimates of incidence and mortality worldwide for 36 cancers in 185 countries. CA Cancer J Clin 71: 209-249, 2021.
3. Huang Z, Sun S, Lee M, Maslov AY, Shi M, Waldman S, Marsh A, Siddiqui T, Dong X, Peter Y, *et al*: Single-cell analysis of somatic mutations in human bronchial epithelial cells in relation to aging and smoking. Nat Genet 54: 492-498, 2022.
4. Pfeifer GP: Smoke signals in the DNA of normal lung cells. Nature 578: 224-226, 2020.
5. Nasim F, Sabath BF and Eapen GA: Lung cancer. Med Clin North Am 103: 463-473, 2019.
6. Bade BC and Dela Cruz CS: Lung Cancer 2020: Epidemiology, etiology, and prevention. Clin Chest Med 41: 1-24, 2020.
7. Liu J, Chen SJ, Hsu SW, Zhang J, Li JM, Yang DC, Gu S, Pinkerton KE and Chen CH: MARCKS cooperates with NKAP to activate NF-kB signaling in smoke-related lung cancer. Theranostics 11: 4122-4136, 2021.
8. Wen J, Fu JH, Zhang W and Guo M: Lung carcinoma signaling pathways activated by smoking. Chin J Cancer 30: 551-558, 2011.
9. Liang Z, Xie W, Wu R, Geng H, Zhao L, Xie C, Li X, Huang C, Zhu J, Zhu M, *et al*: ERK5 negatively regulates tobacco smoke-induced pulmonary epithelial-mesenchymal transition. Oncotarget 6: 19605-19618, 2015.
10. Pastushenko I, Mauri F, Song Y, Cock F, Meeusen B, Swedlund B, Impens F, Van Haver D, Opitz M, Thery M, *et al*: Fat1 deletion promotes hybrid EMT state, tumour stemness and metastasis. Nature 589: 448-455, 2021.
11. Banerjee P, Xiao GY, Tan X, Zheng VJ, Shi L, Rabassedas MNB, Guo HF, Liu X, Yu J, Diao L, *et al*: The EMT activator ZEB1 accelerates endosomal trafficking to establish a polarity axis in lung adenocarcinoma cells. Nat Commun 12: 6354, 2021.
12. Adachi Y, Ito K, Hayashi Y, Kimura R, Tan TZ, Yamaguchi R and Ebi H: Epithelial-to-mesenchymal transition is a cause of both intrinsic and acquired resistance to KRAS G12C inhibitor in KRAS G12C-mutant non-small cell lung cancer. Clin Cancer Res 26: 5962-5973, 2020.
13. Chu S, Ma L, Wu Y, Zhao X, Xiao B and Pan Q: C-EBPβ mediates in cigarette/IL-17A-induced bronchial epithelial-mesenchymal transition in COPD mice. BMC Pulm Med 21: 376, 2021.
14. Chen TY, Liu CH, Chen TH, Chen MR, Liu SW, Lin P and Lin KM: Conditioned media of adipose-derived stem cells suppresses sidestream cigarette smoke extract induced cell death and epithelial-mesenchymal transition in lung epithelial cells. Int J Mol Sci 22: 12069, 2021.
15. Lu L, Chen J, Li M, Tang L, Wu R, Jin L and Liang Z: β-carotene reverses tobacco smoke-induced gastric EMT via Notch pathway *in vivo*. Oncol Rep 39: 1867-1873, 2018.
16. Xie C, Zhu J, Huang C, Yang X, Wang X, Meng Y, Geng S, Wu J, Shen H, Hu Z, *et al*: Interleukin-17A mediates tobacco smoke-induced lung cancer epithelial-mesenchymal transition through transcriptional regulation of ΔNp63α on miR-19. Cell Biol Toxicol 38: 273-289, 2022.
17. Xie C, Zhu J, Yang X, Huang C, Zhou L, Meng Z, Li X and Zhong C: TAp63α is involved in tobacco smoke-induced lung cancer EMT and the anti-cancer activity of curcumin via miR-19 transcriptional suppression. Front Cell Dev Biol 9: 645402, 2021.
18. Su X, Chen J, Lin X, Chen X, Zhu Z, Wu W, Lin H, Wang J, Ye J and Zeng Y: FERMT3 mediates cigarette smoke-induced epithelial-mesenchymal transition through Wnt/β-catenin signaling. Respir Res 22: 286, 2021.
19. Gandhi GR, Antony PJ, Lana MJMP, da Silva BFX, Oliveira RV, Jothi G, Hariharan G, Mohana T, Gan RY, Gurgel RQ, *et al*: Natural products modulating interleukins and other inflammatory mediators in tumor-bearing animals: A systematic review. Phytomedicine 100: 154038, 2022.
20. Tan LTO and Trio-Ranche FKC: Atypical lymphoid proliferation of the orbit. GMS Ophthalmol Cases 12: Doc06, 2022.
21. Mondal P, Mohapatra S, Bhunia D, Gharai PK, Mukherjee N, Gupta V, Ghosh S and Ghosh S: Designed hybrid anticancer nuclear-localized peptide inhibits aggressive cancer cell proliferation. RSC Med Chem 13: 196-201, 2021.
22. Wu JY, Chen YJ, Fu XQ, Li JK, Chou JY, Yin CL, Bai JX, Wu Y, Wang XQ, Li AS, *et al*: Chrysoeriol suppresses hyperproliferation of rheumatoid arthritis fibroblast-like synoviocytes and inhibits JAK2/STAT3 signaling. BMC Complement Med Ther 22: 73, 2022.
23. Irie H, Ozaki M, Chubachi S, Hegab AE, Tsutsumi A, Kameyama N, Sakurai K, Nakayama S, Kagawa S, Wada S, *et al*: Short-term intermittent cigarette smoke exposure enhances alveolar type 2 cell stemness via fatty acid oxidation. Respir Res 23: 41, 2022.
24. Gu W, Wang L, Deng G, Gu X, Tang Z, Li S, Jin W, Yang J, Guo X and Li Q: Knockdown of long noncoding RNA MIAT attenuates cigarette smoke-induced airway remodeling by downregulating miR-29c-3p-HIF3A axis. Toxicol Lett 357: 11-19, 2022.
25. Geng H, Zhao L, Liang Z, Zhang Z, Xie D, Bi L, Wang Y, Zhang T, Cheng L, Yu D and Zhong C: Cigarette smoke extract-induced proliferation of normal human urothelial cells via the MAPK/AP-1 pathway. Oncol Lett 13: 469-475, 2017.
26. Rovida E and Tusa I: Targeting MAPK in cancer 2.0. Int J Mol Sci 23: 5702, 2022.
27. Caeser R, Hulton C, Costa E, Durani V, Little M, Chen X, Tischfield SE, Asher M, Kombak FE, Chavan SS, *et al*: MAPK pathway activation selectively inhibits ASCL1-driven small cell lung cancer. iScience 24: 103224, 2021.
28. Wang B, Zhuang R, Luo X, Yin L, Pang C, Feng T, You H, Zhai Y, Ren Y, Zhang L, *et al*: Prevalence of metabolically healthy obese and metabolically obese but normal weight in adults worldwide: A meta-analysis. Horm Metab Res 47: 839-845, 2015.
29. Okada T, Sinha S, Esposito I, Schiavon G, López-Lago MA, Su W, Pratilas CA, Abele C, Hernandez JM, Ohara M, *et al*: The Rho GTPase Rnd1 suppresses mammary tumorigenesis and EMT by restraining Ras-MAPK signalling. Nat Cell Biol 17: 81-94, 2015.
30. Kang J, Park JH, Kong JS, Kim MJ, Lee SS, Park S and Myung JK: PINX1 promotes malignant transformation of thyroid cancer through the activation of the AKT/MAPK/β-catenin signaling pathway. Am J Cancer Res 11: 5485-5495, 2021.

31. Kumar D, Patel SA, Hassan MK, Mohapatra N, Pattanaik N and Dixit M: Reduced IQGAP2 expression promotes EMT and inhibits apoptosis by modulating the MEK-ERK and p38 signaling in breast cancer irrespective of ER status. Cell Death Dis 12: 389, 2021.
32. Zhu N, Zhang XJ, Zou H, Zhang YY, Xia JW, Zhang P, Zhang YZ, Li J, Dong L, Wumaier G and Li SQ: PTPL1 suppresses lung cancer cell migration via inhibiting TGF-β1-induced activation of p38 MAPK and Smad 2/3 pathways and EMT. Acta Pharmacol Sin 42: 1280-1287, 2021.
33. Shu L, Chen S, Lin S, Lin H, Shao Y, Yao J, Qu L, Zhang Y, Liu X, Du X, *et al*: The pseudomonas aeruginosa secreted protein PA3611 promotes bronchial epithelial cell epithelial-mesenchymal transition via integrin αvβ6-mediated TGF-β1-induced p38/NF-κB pathway activation. Front Microbiol 12: 763749, 2022.
34. Li S, Wang H, Ma R and Wang L: Schisandrin B inhibits epithelial-mesenchymal transition and stemness of large-cell lung cancer cells and tumorigenesis in xenografts via inhibiting the NF-κB and p38 MAPK signaling pathways. Oncol Rep 45: 115, 2021.
35. Liang Z, Wu R, Xie W, Zhu M, Xie C, Li X, Zhu J, Zhu W, Wu J, Geng S, *et al*: Curcumin reverses tobacco smoke-induced epithelial-mesenchymal transition by suppressing the MAPK pathway in the lungs of mice. Mol Med Rep 17: 2019-2025, 2018.
36. Saxena A, Walters MS, Shieh JH, Shen LB, Gomi K, Downey RJ, Crystal RG and Moore MAS: Extracellular vesicles from human airway basal cells respond to cigarette smoke extract and affect vascular endothelial cells. Sci Rep 11: 6104, 2021.
37. Lu Q, Lai Y, Zhang H, Ren K, Liu W, An Y, Yao J and Fan H: Hesperetin inhibits TGF-β1-induced migration and invasion of triple negative breast cancer MDA-MB-231 cells via suppressing Fyn/Paxillin/RhoA pathway. Integr Cancer Ther 21: 15347354221086900, 2022.
38. Ricci A, Gallorini M, Del Bufalo D, Cataldi A, D'Agostino I, Carradori S and Zara S: Negative modulation of the angiogenic cascade induced by allosteric kinesin Eg5 inhibitors in a gastric adenocarcinoma in vitro model. Molecules 27: 957, 2022.
39. Wang SW, Sheng H, Zheng F and Zhang F: Hesperetin promotes DOT1L degradation and reduces histone H3K79 methylation to inhibit gastric cancer metastasis. Phytomedicine 84: 153499, 2021.
40. Zhang J, Wu D, Vikash, Song J, Wang J, Yi J and Dong W: Hesperetin induces the apoptosis of gastric cancer cells via activating mitochondrial pathway by increasing reactive oxygen species. Dig Dis Sci 60: 2985-2995, 2015.
41. Semis HS, Kandemir FM, Kaynar O, Dogan T and Arikan SM: The protective effects of hesperidin against paclitaxel-induced peripheral neuropathy in rats. Life Sci 287: 120104, 2021.
42. Zhou L, Gu W, Kui F, Gao F, Niu Y, Li W, Zhang Y, Guo L, Wang J, Guo Z and Du G: The mechanism and candidate compounds of aged citrus peel (chenpi) preventing chronic obstructive pulmonary disease and its progression to lung cancer. Food Nutr Res 65, 2021.
43. Kong W, Ling X, Chen Y, Wu X, Zhao Z, Wang W, Wang S, Lai G and Yu Z: Hesperetin reverses P-glycoprotein-mediated cisplatin resistance in DDP-resistant human lung cancer cells via modulation of the nuclear factor-κB signaling pathway. Int J Mol Med 45: 1213-1224, 2020.
44. Hu G, Cao C, Deng Z, Li J, Zhou X, Huang Z and Cen C: Effects of matrine in combination with cisplatin on liver cancer. Oncol Lett 21: 66, 2021.
45. Zhang B, Gong A, Shi H, Bie Q, Liang Z, Wu P, Mao F, Qian H and Xu W: Identification of a novel YAP-14-3-3ζ negative feedback loop in gastric cancer. Oncotarget 8: 71894-71910, 2017.
46. Livak KJ and Schmittgen TD: Analysis of relative gene expression data using real-time quantitative PCR and the 2(-Delta Delta C(T)) method. Methods 25: 402-408, 2001.
47. Lu L, Chen J, Tang H, Bai L, Lu C, Wang K, Li M, Yan Y, Tang L, Wu R, *et al*: EGCG suppresses ERK5 activation to reverse tobacco smoke-triggered gastric epithelial-mesenchymal transition in BALB/c mice. Nutrients 8: 380, 2016.
48. Lu L, Liang Q, Shen S, Feng L, Jin L and Liang ZF: Tobacco smoke plays an important role in initiation and development of lung cancer by promoting the characteristics of cancer stem cells. Cancer Manag Res 12: 9735-9739, 2020.
49. Intlekofer AM and Finley LWS: Metabolic signatures of cancer cells and stem cells. Nat Metab 1: 177-188, 2019.
50. Liang Z, Wu R, Xie W, Xie C, Wu J, Geng S, Li X, Zhu M, Zhu W, Zhu J, *et al*: Effects of curcumin on tobacco smoke-induced hepatic MAPK pathway activation and epithelial-mesenchymal transition in vivo. Phytother Res 31: 1230-1239, 2017.
51. Liang Z, Lu L, Mao J, Li X, Qian H and Xu W: Curcumin reversed chronic tobacco smoke exposure induced urocystic EMT and acquisition of cancer stem cells properties via Wnt/β-catenin. Cell Death Dis 8: e3066, 2017.
52. Terry S, Savagner P, Ortiz-Cuaran S, Mahjoubi L, Saintigny P, Thiery JP and Chouaib S: New insights into the role of EMT in tumor immune escape. Mol Oncol 11: 824-846, 2017.
53. Jang HR, Shin SB, Kim CH, Won JY, Xu R, Kim DE and Yim H: PLK1/vimentin signaling facilitates immune escape by recruiting Smad2/3 to PD-L1 promoter in metastatic lung adenocarcinoma. Cell Death Differ 28: 2745-2764, 2021.
54. Bai X, Wei H, Liu W, Coker OO, Gou H, Liu C, Zhao L, Li C, Zhou Y, Wang G, *et al*: Cigarette smoke promotes colorectal cancer through modulation of gut microbiota and related metabolites. Gut 71: 2439-2450, 2022.
55. Jia Y, Zhang Q, Liu Z, Pan P, Jia Y, Zhu P, Jiao Y, Kang G and Ma X: The role of α5-nicotinic acetylcholine receptor/NLRP3 signaling pathway in lung adenocarcinoma cell proliferation and migration. Toxicology 469: 153120, 2022.
56. Agraval H, Sharma JR, Prakash N and Yadav UCS: Fisetin suppresses cigarette smoke extract-induced epithelial to mesenchymal transition of airway epithelial cells through regulating COX-2/MMPs/β-catenin pathway. Chem Biol Interact 351: 109771, 2022.
57. Zhang J, Chang Y, Xia H, Xu L and Wei X: HIST1H2BN induced cell proliferation and EMT phenotype in prostate cancer via NF-κB signal pathway. Genes Genomics 43: 1361-1369, 2021.
58. Xueqin T, Jinhong M and Yuping H: Inhibin subunit beta A promotes cell proliferation and metastasis of breast cancer through Wnt/β-catenin signaling pathway. Bioengineered 12: 11567-11575, 2021.
59. Yang M, Jin M, Li K, Liu H, Yang X, Zhang X, Zhang B, Gong A and Bie Q: TRAF6 promotes gastric cancer cell self-renewal, proliferation, and migration. Stem Cells Int 2020: 3296192, 2020.
60. Drosten M and Barbacid M: Targeting the MAPK pathway in KRAS-driven tumors. Cancer Cell 37: 543-550, 2020.
61. Lee S, Rauch J and Kolch W: Targeting MAPK signaling in cancer: Mechanisms of drug resistance and sensitivity. Int J Mol Sci 21: 1102, 2020.
62. Arora A, Bhuria V, Singh S, Pathak U, Mathur S, Hazari PP, Roy BG, Sandhir R, Soni R, Dwarakanath BS and Bhatt AN: Amifostine analog, DRDE-30, alleviates radiation induced lung damage by attenuating inflammation and fibrosis. Life Sci 298: 120518, 2022.
63. Xie X, Deng T, Duan J, Xie J, Yuan J and Chen M: Exposure to polystyrene microplastics causes reproductive toxicity through oxidative stress and activation of the p38 MAPK signaling pathway. Ecotoxicol Environ Saf 190: 110133, 2020.
64. Sanit J, Prompunt E, Adulyaritthikul P, Nokkaew N, Mongkolpathumrat P, Kongpol K, Kijtawornrat A, Petchdee S, Barrère-Lemaire S and Kumphune S: Combination of metformin and p38 MAPK inhibitor, SB203580, reduced myocardial ischemia/reperfusion injury in non-obese type 2 diabetic Goto-Kakizaki rats. Exp Ther Med 18: 1701-1714, 2019.
65. Yamamoto S, Lee S, Ariyasu T, Endo S, Miyata S, Yasuda A, Harashima A, Ohta T, Kumagai-Takei N, Ito T, *et al*: Ingredients such as trehalose and hesperidin taken as supplements or foods reverse alterations in human T cells, reducing asbestos exposure-induced antitumor immunity. Int J Oncol 58: 2, 2021.
66. Deng J, Liu L, Li L, Sun J and Yan F: Hesperidin delays cell cycle progression into the G0/G1 phase via suspension of MAPK signaling pathway in intrahepatic cholangiocarcinoma. J Biochem Mol Toxicol 36: e22981, 2022.